nature chemical biology

ARTICLE

PUBLISHED ONLINE: 3 APRIL 2011 | DOI: 10.1038/NCHEMBIO.552

Cannabinoid potentiation of glycine receptors contributes to cannabis-induced analgesia

Wei Xiong[1], KeJun Cheng[2], Tanxing Cui[3–5], Grzegorz Godlewski[6], Kenner C Rice[2], Yan Xu[3–5] & Li Zhang[1]*

Cannabinoids enhance the function of glycine receptors (GlyRs). However, little is known about the mechanisms and behavioral implication of cannabinoid-GlyR interaction. Using mutagenesis and NMR analysis, we have identified a serine at 296 in the GlyR protein critical for the potentiation of I_{Gly} by Δ^9-tetrahydrocannabinol (THC), a major psychoactive component of marijuana. The polarity of the amino acid residue at 296 and the hydroxyl groups of THC are critical for THC potentiation. Removal of the hydroxyl groups of THC results in a compound that does not affect I_{Gly} when applied alone but selectively antagonizes cannabinoid-induced potentiating effect on I_{Gly} and analgesic effect in a tail-flick test in mice. The cannabinoid-induced analgesia is absent in mice lacking α3GlyRs but not in those lacking CB1 and CB2 receptors. These findings reveal a new mechanism underlying cannabinoid potentiation of GlyRs, which could contribute to some of the cannabis-induced analgesic and therapeutic effects.

Cannabis attracts broad scientific interest because it produces both beneficial and harmful effects on human health[1]. Cannabis is composed of more than 400 chemical components. A number of these components are found to provide therapeutic relief in alleviating chronic pain, seizure, depression and muscle spasms resulting from multiple sclerosis[1], but the primary psychoactive ingredient in cannabis, Δ^9-tetrahydrocannabinol (**1**, THC), produces some unwanted effects on human health, such as motor impairment and psychosis. Although most THC-induced central effects are mediated through the activation of a cannabinoid type 1 (CB1) receptor, evidence has emerged to suggest that some of the THC-induced cellular and behavioral effects are independent of CB1 receptors[2–4]. For instance, intrathecal injection of a selective CB1 antagonist cannot completely inhibit the analgesic effects induced by THC and deoxy-HU 210 (**2**), a synthetic cannabinoid structurally similar to THC, in spinal tail-flick reflex test (TFR) in mice[5]. THC-induced analgesia in the TFR remains intact in mice with depleted CB1 receptors ($CB1^{-/-}$)[2]. There are indications from very recent studies that endogenous CB1 receptors may play a pronociceptive role instead of an antinociceptive role in spinal dorsal horn, an area critical for pain sensory formation[6,7]. A number of nonpsychoactive cannabinoids structurally similar to THC are found to exert neuroprotection, antiemetic and antinociceptive effects[8,9]. Although the therapeutic potential of nonpsychotropic cannabinoids has been the topic of interest over the last several decades[9], relatively less is known about the molecular sites and mechanisms that mediate nonpsychoactive cannabinoid-induced actions.

Emerging evidence has suggested that inhibitory glycine receptors (GlyRs) are an important target for cannabis in the central and peripheral nervous systems[4,10]. THC and other cannabinoids can increase the activity of native and recombinant GlyRs through a CB1- and CB2-independent mechanism[10–12]. THC and GlyRs share similar roles in regulation of some behaviors, such as neuromotor activity, pain sensation, muscle relaxation and anxiety[1,13]. Humans and rodents carrying single amino acid mutations on the α1 GlyRs at postsynaptic sites have severe deficiency in neuromotor activity[14,15]. The α3 GlyRs are abundantly expressed in the adult spinal cord dorsal horn where these receptors critically regulate inflammatory pain sensation[16]. Nevertheless, the idea that the GlyRs are an important target for cannabinoids has been largely ignored because our knowledge is limited regarding the mechanisms and behavioral implication of cannabinoid potentiation of GlyRs. Here we identify a new mechanism by which THC potentiates GlyRs. We also provide evidence to suggest that the site and the action of mechanism of cannabinoid potentiation of GlyRs critically contribute to the cannabis-induced analgesic effect. These findings could help to identify a new strategy for developing analgesic agents.

RESULTS

THC potentiation of native and recombinant GlyRs

THC at relatively low concentrations enhanced I_{Gly} in cultured spinal neurons (**Fig. 1a**). The magnitudes of the potentiating effect on I_{Gly} induced by 30 nM, 100 nM and 300 nM THC were 44 ± 13%, 82 ± 4% and 136 ± 11%. THC-induced potentiating effect on I_{Gly} developed gradually with continuous application of THC for 5 min in both cultured spinal neurons and HEK 293 cells expressing the α1 and α1β1 GlyR subunits (**Fig. 1b**). The peak amplitude of THC potentiation was nearly ten-fold higher than the initial value of THC potentiation. It is well accepted that the native GlyRs in adult brains are formed by the α- and β-subunits[17]. Consistent with this, the sensitivities of the native and heteromeric α1β1 GlyRs to THC were nearly identical but were significantly less than that of the homomeric α1 receptors. In addition to activating CB1 and CB2 receptors, THC is found to directly activate vanilloid receptors in rat trigeminal neurons[18]. In this regard, we examined whether CB1, CB2 and vanilloid receptors are involved in THC potentiation of GlyRs. Selective antagonists of CB1 (AM251 **3**, 2 μM), CB2 (SR144528 **4**, 2 μM) and vanilloid (capsazepine **5**, 2 μM) receptors

[1]Laboratory for Integrative Neuroscience, US National Institute on Alcohol Abuse and Alcoholism, US National Institutes of Health, Bethesda, Maryland, USA. [2]Chemical Biological Research Branch, US National Institute on Drug Abuse, US National Institutes of Health, Bethesda, Maryland, USA. [3]Department of Anesthesiology, University of Pittsburgh School of Medicine, Pittsburgh, Pennsylvania, USA. [4]Department of Pharmacology and Chemical Biology, University of Pittsburgh School of Medicine, Pittsburgh, Pennsylvania, USA. [5]Department of Structural Biology, University of Pittsburgh School of Medicine, Pittsburgh, Pennsylvania, USA. [6]Laboratory of Physiologic Studies, US National Institute on Alcohol Abuse and Alcoholism, US National Institutes of Health, Bethesda, Maryland, USA. *e-mail: lzhang@mail.nih.gov

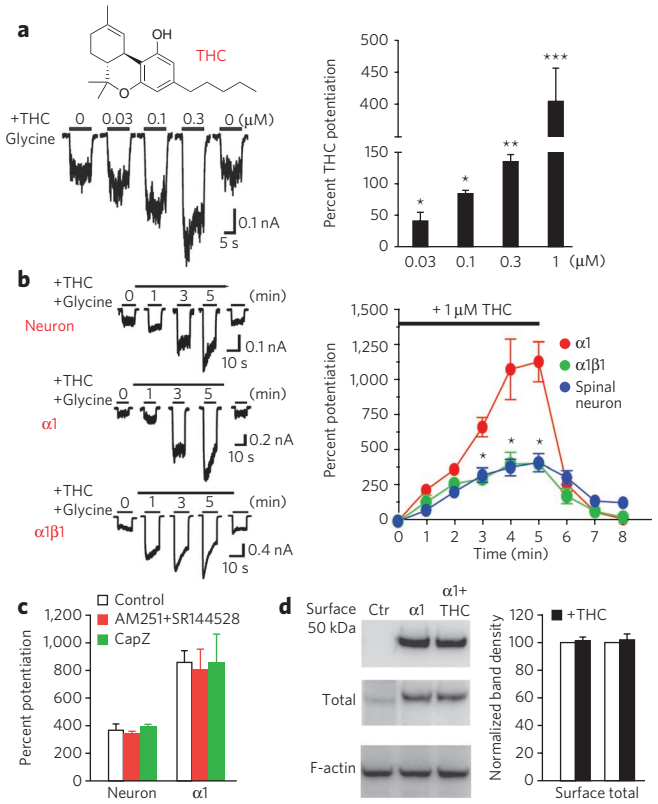

Figure 1 | THC potentiation of I_{Gly}. (**a**) Chemical structure of THC. Trace records of I_{Gly} activated by a 2% maximal effective concentration (EC_2) (10 μM) before and after a 5-min continuous incubation with THC in cultured spinal neurons. Bar graphs of THC-induced potentiating effect on I_{Gly}. $^*P < 0.05$, $^{**}P < 0.01$, $^{***}P < 0.001$, unpaired *t*-test, as compared with I_{Gly} without THC (n = 6–9). (**b**) Trace records of I_{Gly} during a 5-min period of continuous incubation with THC (1 μM). Time course of average percentage potentiation induced by 1 μM THC during a 5-min period of continuous incubation. The solid bar indicates THC application time. Each point represents mean ± s.e.m. of at least 7 cells. $^*P < 0.05$, based on repeated measures of analysis of variance (ANOVA), as compared to α1 subunit (n = 6–11). (**c**) The effects of AM251, SR144528 and capsazepine (CapZ) on THC potentiation ($P > 0.1$, ANOVA, n = 7). (**d**) Western blot of total and surface proteins of the α1 subunits expressed in HEK 293 cells. Normalized band intensity of the surface and total proteins of the α1 GlyRs in the absence (open bars) and presence of THC (solid bars). ($P > 0.1$, unpaired *t*-test, n = 3).

did not significantly alter the THC-induced potentiating effect on I_{Gly} in both spinal neurons and HEK 293 cells expressing the α1 GlyRs (**Fig. 1c**). THC is unlikely to alter GlyR trafficking, as there was no apparent difference in the levels of total and surface α1 GlyR proteins in the absence and presence of THC detected by immunoblot (**Fig. 1d** and **Supplementary Results**, **Supplementary Fig. 6**).

Ser296 is a distinct site essential for THC potentiation

To localize molecular domains of GlyRs that mediate THC potentiation, we first examined whether THC can differentially affect three distinct α-subunits of GlyRs. Although the α1 and α3 GlyR subunits appeared to be equally sensitive to the THC-induced potentiating effect, the α2 GlyR subunits were significantly less sensitive to THC when expressed in HEK 293 cells (**Fig. 2a–c**). The magnitudes of average percent potentiation induced by 1 μM THC were 1,156 ± 472% and 1,127 ± 142% in cells expressing the α1 and α3 subunits. In contrast, the magnitude of THC potentiation of the α2 subunit was 232 ± 35% (**Fig. 2b**). The maximal efficacy of THC in potentiating I_{Gly} was also significantly less in the cells expressing the α2 subunits than the cells expressing the α1 and α3 subunits (**Fig. 2c**). A recent study has shown that CP55940 (**6**), a synthetic CB1 agonist structurally similar to THC, was exclusively concentrated in the membrane lipid matrix where CP55940 could access to the binding pockets in the receptor transmembrane domains[19]. In view of this finding, we focused on the transmembrane domains of GlyRs in looking for potential molecular determinants of THC potentiation. Alignment of the amino acid sequence of all four transmembrane domains across three α subunits revealed a serine residue at 296 in the transmembrane domain 3 (TM3) that is identical in the α1 and α3 subunits but not in the α2 subunit (**Fig. 2d**). Aligned with Ser296 in the α1 subunit is Ala303 in the α2 subunit. Throughout the entire four transmembrane domains, Ala303 is the only residue that differs from both of the equivalent residues (Ser296 and Ser307) in the α1 and α3 subunits. Substitution of Ser296 in the α1 subunit with an alanine significantly reduced the maximal magnitude of THC potentiation by nearly 80% and resulted in a concentration response curve of THC potentiation identical to that of the α2 subunits (**Fig. 2e**). A similar scenario also occurred in the α3 subunit where the substitution of Ser307 with an alanine significantly reduced the sensitivity of the α3 subunit to THC (**Fig. 2f**). Conversely, substitution of the corresponding residue, Ala303, of the α2 subunit with a serine converted the α2 subunit from a receptor with a low THC sensitivity to a high THC sensitivity (**Supplementary Fig. 1a**). It is worth mentioning that, similar to our observation in neurons, THC at low concentrations (30–300 nM) significantly enhanced I_{Gly} in HEK 293 cells expressing the α1 and α3 subunits. The S296A and S307A mutations significantly reduced the magnitude of the potentiation induced by low concentrations of THC. For instance, the extents of the potentiating effect induced by 100 nM THC were 97 ± 7% and 23 ± 4% in cells expressing the wild-type and S307A mutant α3 subunits ($P < 0.01$, unpaired *t*-test, n = 6). The point mutations of S296A in the α1 subunit, A303S in the α2 subunit and S307A in the α3 subunit did not significantly affect the half-maximal effective concentration (EC_{50}) values of the GlyRs (**Supplementary Fig. 1b**). The S296A mutation of the α1 subunit did not significantly affect propofol (**7**)-, trichloroethanol (**8**)-, etomidate (**9**)- and ethanol (**10**)-induced potentiation, suggesting that the Ser296 is a distinct site for THC-induced action (**Supplementary Fig. 1c**,**d**).

NMR: THC induces a chemical shift of Ser296

Next we carried out NMR chemical shift measurements to determine whether or not THC directly interacts with the transmembrane domains of GlyR. The proteins of the full-length transmembrane domains of the human α1 GlyR were overexpressed and purified using Rosetta (DE3) pLysS–competent *E. coli* cells as described in Methods and **Supplementary Methods**. Molecular modeling of the four transmembrane domains of the α1 subunit reveals the specific location of Ser296 in green (**Fig. 3a**). Titration of THC to the transmembrane domains of the human α1 GlyR subunit (GlyR-TM) reconstituted in lyso-1-palmitoylphosphphotidylglycerol (LPPG) micelles showed that most of the resonances of the transmembrane domains in the 2D ^{15}N heteronuclear single quantum coherence (HSQC) spectra remained unchanged after the addition of THC, suggesting that the interaction between THC and GlyR-TM does not alter the overall structure of GlyR-TM. However, the resonance of Ser296 was highly sensitive to THC (**Fig. 3b**). We next tested the effect of ethanol on the resonance of Ser296 because ethanol was used as a solvent to dissolve THC. Ethanol alone caused a Ser296 resonance shift in the up field direction (**Fig. 3c**). In contrast, the Ser296 resonance shifted steeply in the downfield direction, showing a high sensitivity to THC (**Fig. 3d**, green and pink open circles). The titration curves showed two distinct concentration dependences at low and high ligand-to-protein ratios (**Fig. 3e**). At low ligand-to-protein ratios (0–17 μM of THC titrated to 450 μM of protein), the

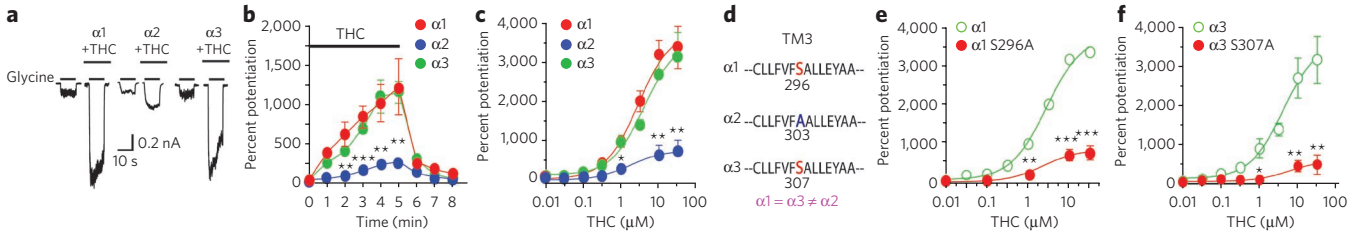

Figure 2 | A distinct site of Ser296 is critical for THC potentiation of the α1 and α3 GlyRs. (**a**) The effect of THC (1 μM) on I_{Gly} activated by EC_2 concentrations of glycine (10 μM for the α1 subunit, 20 μM for the α2 subunit and 100 μM for the α3 subunit) in HEK 293 cells. (**b**) Time course of THC (1 μM) potentiation of I_{Gly} in cells expressing different α subunits. The solid bar indicates the time of THC application. $^{**}P < 0.01$, $^{***}P < 0.001$, using ANOVA against α1 ($n = 7$). (**c**) The concentration response curves of THC potentiation of I_{Gly} in cells expressing different α subunits. $^{*}P < 0.05$, $^{**}P < 0.01$, using ANOVA against α1 ($n = 7$–9). (**d**) Amino acid alignment of the TM3 region flanking Ser296 (α1) or equivalent residues in the α2 and α3 subunits. (**e**) The concentration response curves of THC potentiation in cells expressing the wild-type (α1) and S296A mutant receptors. $^{**}P < 0.01$, $^{***}P < 0.001$, ANOVA against α1 ($n = 7$–9). (**f**) The concentration response curves of THC potentiation in cells expressing the wild-type (α3) and S307A mutant receptors. $^{*}P < 0.05$, $^{**}P < 0.01$, ANOVA against α3 ($n = 5$–6).

Ser296 resonance shifted steeply in the downfield direction, showing a hypersensitivity to THC (green and pink solid circles). This is a strong indication that THC interacts selectively with Ser296. At higher ligand-to-protein ratios, a typical saturation curve was observed. The discontinuity in the THC titration curve at the high concentration range is likely due to the interfering effect induced by ethanol. The amount of ethanol increased dramatically (up to 86 mM) when titrated in the range with high ligand-to-protein ratio. It is possible that ethanol, especially at high concentrations, may inhibit the interaction between THC and Ser296 under the NMR experimental conditions. There were a few peaks that were slightly modified in the presence of high concentrations of THC (>90 μM). These peaks arose from the residues in an artificial flexible linker engineered to connect TM3 with TM4 or in a C-terminal His tag.

Evidence for a hydrogen bond–like interaction

To further explore the molecular insight into the role of Ser296 in THC-induced potentiation of GlyRs, we used mutagenesis to analyze the interrelationship between THC potentiation and the biophysical properties of the amino acid residues at 296 and 307 of the α1 and α3 subunits. The sensitivity of the mutant receptors to the THC-induced potentiating effect on I_{Gly} varied substantially (**Fig. 4a**). There was a strong correlation between the polarity of the amino acid residue at 296 α1 or 307 α3 and THC potentiation of the α1 and α3 subunits ($r^2 = 0.608$, $r^2 = 0.768$, **Fig. 4b**,**c**). In contrast, the magnitude of THC potentiation was not significantly correlated with the volume of the residue at 296, the glycine EC_{50} value and mean current density of the wild-type and mutant receptors (**Fig. 4d**–**f**). These observations suggest that THC is likely to interact with Ser296 of GlyRs via a hydrogen bond interaction. To further test this hypothesis, we chemically modified THC by removing the hydroxyl, oxygen or both groups from the THC (see detailed procedure of chemical synthesis in **Supplementary Methods**). The resulting chemicals are named as follows: 5-desoxy-THC (**11**), 1-desoxy-THC (**12**) and di-desoxy-THC (**13**, DiDe-THC) (**Supplementary Fig. 2**). Chemical modification of THC significantly reduced the binding affinity of 5-desoxy-THC and 1-desoxy-THC to CB1 but not to CB2 receptors (**Fig. 5a**,**b**). In contrast, di-desoxy-THC with both hydroxyl and oxygen groups removed completely lost the binding affinity for both CB1 and CB2 receptors. Di-desoxy-THC and 5-desoxy-THC did not stimulate [^{35}S]-GTPγs binding when applied alone nor did they alter CP55940- and THC-induced stimulation of [^{35}S]-GTPγs binding in brain plasma membranes (**Fig. 5c**). Although 5-desoxy-THC and 1-desoxy-THC potentiated I_{Gly} in a manner similar to THC, di-desoxy-THC was nearly ineffective in potentiating I_{Gly} (**Fig. 5d**). However, di-desoxy-THC significantly inhibited the THC-induced potentiating effect on I_{Gly} (**Fig. 5e**). Di-desoxy-THC did not significantly affect the potentiating effect on I_{Gly} induced by 100 μM propofol (**Fig. 5f**), suggesting that di-desoxy-THC selectively antagonizes the THC-induced potentiating effect.

The α3 GlyRs: essential for cannabis-induced analgesia

The above observations suggest that using both 5-desoxy-THC and di-desoxy-THC could be valuable approaches for identifying the behavioral consequence of THC potentiation of GlyRs *in vivo*. A previous study has shown that the THC-induced analgesic effect in the TFR remained unchanged in $CB1^{-/-}$ and $CB1^{-/-}$-$CB2^{-/-}$ double-knockout mice[2]. In view of this observation, we asked

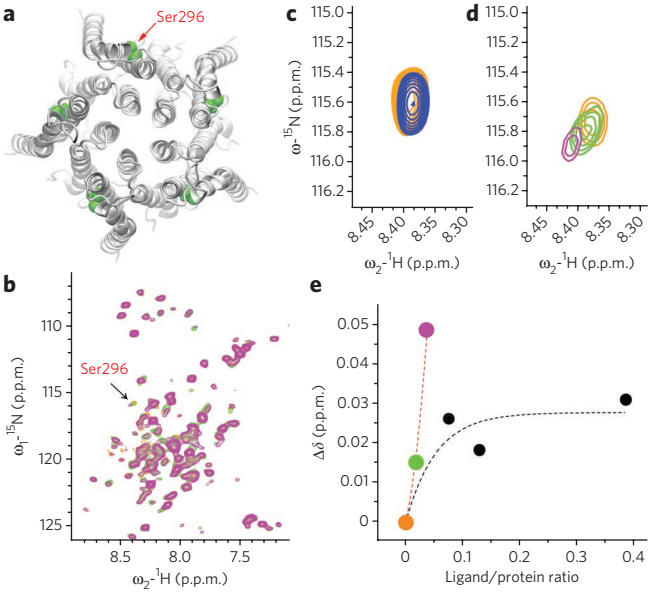

Figure 3 | NMR analysis. (**a**) Molecular modeling of the four transmembrane domains of the α1 GlyR protein. (**b**) The essential data sets covering all ^{15}N-^{1}H HSQC resonances from the residues in the GlyR transmembrane domains. Three representative HSQC spectra of 450 μM GlyR-TM titrated by 0 μM (orange), 8.5 μM (green) and 17 μM (pink) THC indicated that Ser296 is sensitive to THC. (**c**) In the absence (orange) and presence (blue) of 0.2% (v/v) ethanol in 250 μM GlyR-TM, the peak of Ser296 is shifted to the upfield. (**d**) Zoom-in view of Ser296 resonance from **b**. (**e**) Observed chemical shift changes ($\Delta\delta$) as a function of the ligand (THC)-to-protein (GlyR-TM) concentration ratio (colored solid circles, low ligand-to-protein ratio; black filled circles, high ligand-to-protein ratio).

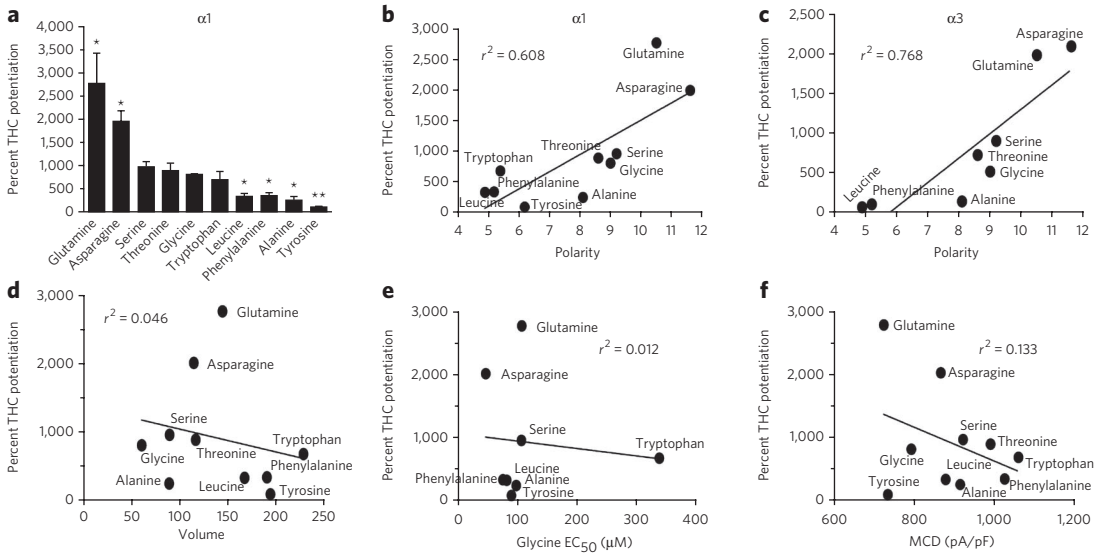

Figure 4 | Mutagenesis and correlation analysis. (**a**) The bar graphs showing average percentage of THC (1 μM) potentiation of the α1 GlyRs carrying various substitutions at 296. *P < 0.05, **P < 0.01, one-way ANOVA and Dunnett's *post hoc* test against wild type (n = 7–11). (**b**) A correlation between the polarity of the residue at 296 of the α1 subunit and the magnitude of THC potentiation. (**c**) A correlation between the polarity of the residue at 296 of the α3 subunit and the magnitude of THC potentiation. (**d**) Correlation analysis of THC potentiation with the volume of the side chain of the residue at 296 of mutant and wild-type α1 GlyRs. (**e**) Correlation analysis of THC potentiation with the EC_{50} values of the glycine concentration response curves of the mutant and wild-type α1 GlyRs. (**f**) Correlation analysis of THC potentiation with the mean current density (MCD) of I_{Gly} in cells expressing the mutant and wild-type α1 GlyRs.

whether or not GlyRs are involved in THC-induced analgesia in the TFR. Both THC and 5-desoxy-THC increased response latencies in the TFR in C57BL/6J mice (**Fig. 6a**). The analgesic effects of THC and 5-desoxy-THC were completely abolished by administration of strychnine (**14**), a selective GlyR antagonist, and di-desoxy-THC but not by a selective CB1 receptor antagonist AM251. We next tested the effect of THC in the TFR in the α3 GlyR subunit knockout mice ($\alpha3^{-/-}$). The baseline of response latency was slightly increased in the TFR in $\alpha3^{-/-}$ mice. The analgesic effect of THC and 5-desoxy-THC was significantly reduced in heterozygous $\alpha3^{+/-}$ mice and completely absent in $\alpha3^{-/-}$ mice (**Fig. 6b**). In contrast, both THC- and 5-desoxy-THC–produced analgesia remained unchanged in $CB1^{-/-}$ and $CB2^{-/-}$ mice as compared to the wild-type littermates (**Fig. 6c,d**). The magnitude of THC-induced and 5-desoxy-THC–induced analgesia increased with increasing drug concentrations up to 50 mg kg^{-1} (**Supplementary Fig. 3a,b**). The analgesic

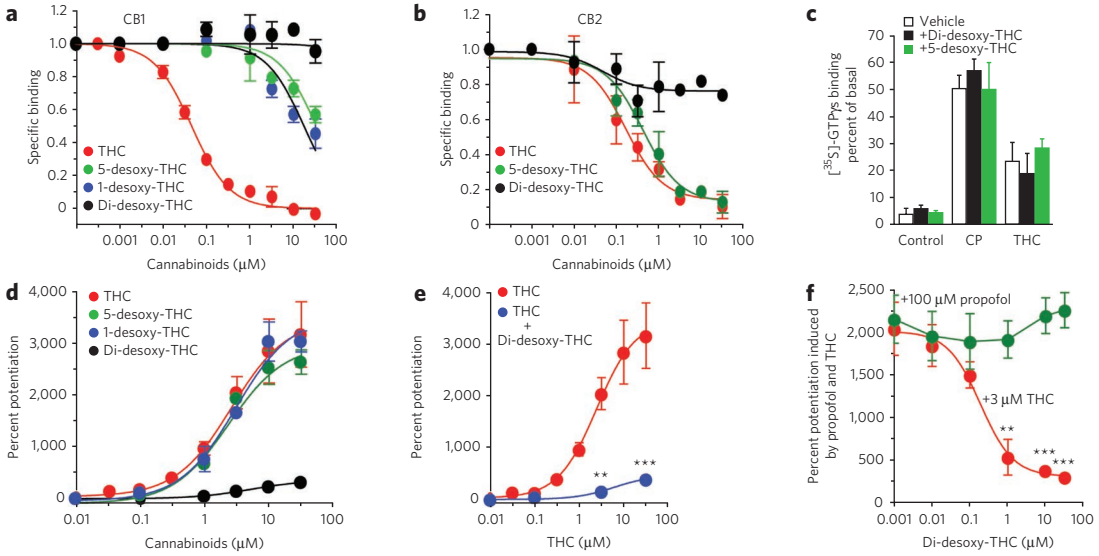

Figure 5 | Functional characterization of 5-desoxy-THC and di-desoxy-THC. (**a**) The concentration response curves of THC, 5-desoxy-THC, 1-desoxy-THC and di-desoxy-THC in suppressing specific binding of [^{3}H]-CP55940 in purified brain membranes. (**b**) The concentration response curves of THC, 5-desoxy-THC and di-desoxy-THC in suppressing specific binding of [^{3}H]-CP55940 in purified membranes from *E. coli* recombinant cells expressing human CB2 receptors. (**c**) The effect of di-desoxy-THC and 5-desoxy-THC on THC- and CP55940-induced stimulation of [^{35}S]-GTPγs binding in purified brain membranes. (**d**) The concentration response curves of cannabinoid potentiation of I_{Gly} in HEK 293 cells expressing the α1 GlyRs. (**e**) Inhibition of THC potentiation by di-desoxy-THC at 10 μM. **P < 0.01, ***P < 0.001, unpaired t-test as compared with control (THC alone) (n = 6–7 for each). (**f**) Di-desoxy-THC, in a concentration-dependent manner, suppresses the potentiating effect on I_{Gly} induced by THC but not propofol, **P < 0.01, ***P < 0.001, based on repeated measures of ANOVA against the point of 0.001 μM di-desoxy-THC (n = 5–7).

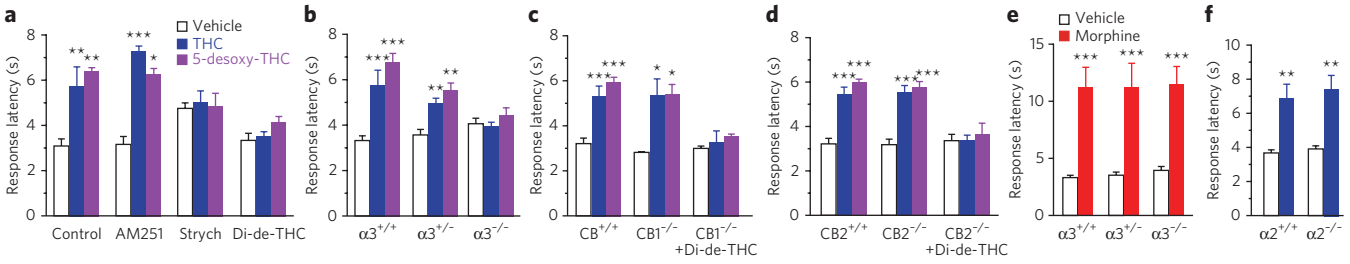

Figure 6 | The critical role of the α3 GlyR in the THC analgesia in the TFR. (**a**) The effects of AM251 (3 mg kg^{-1}, i.p.), strychnine (strych, 0.2 mg kg^{-1}, s.c.) and di-desoxy-THC (Di-de-THC: 20 mg kg^{-1}, i.p.) on THC at 10 mg kg^{-1}, i.p. and 5-desoxy-THC at 10 mg kg^{-1}, i.p. induced analgesia in the TFR. *P < 0.05, **P < 0.01, ***P < 0.001, based on one-way ANOVA and Dunnett's *post hoc* test against control group (n = 11–12 for each). (**b**) The analgesic effect of THC and 5-desoxy-THC in the TFR in the wild-type litter mates (α3$^{+/+}$), heterozygotes (α3$^{+/-}$) and homozygotes (α3$^{-/-}$) of α3 GlyR-KO mice. **P < 0.01, ***P < 0.001 (n = 5–7). (**c**) The analgesic effect of THC and 5-desoxy-THC in the TFR in CB1$^{+/+}$ and CB1$^{-/-}$ mice without and with administration of di-desoxy-THC. *P < 0.05, ***P < 0.001 (n = 6). (**d**) The analgesic effect of THC and 5-desoxy-THC on tail-flick test in CB2$^{-/-}$ mice without and with administration of di-desoxy-THC. ***P < 0.001 (n = 6). (**e**) The analgesic effect of morphine at 10 mg kg^{-1}, i.p. in the TFR in α3$^{+/+}$, α3$^{+/-}$ and α3$^{-/-}$ mice. ***P < 0.001 (n = 7). (**f**) The analgesic effect of THC in the TFR in wild-type littermates (α2$^{+/+}$) and homozygotes (α2$^{-/-}$) of α2 GlyR-KO mice. **P < 0.01 (n = 6).

effect induced by various doses of THC did not significantly differ between the wild-type and CB1$^{-/-}$ mice (**Supplementary Fig. 3a**). In contrast, the analgesic effect of THC at 30 mg–50 mg kg^{-1}, intraperitoneal (i.p.) injection, in the TFR was either absent or substantially reduced by 80% in the α3$^{-/-}$ mice as compared with the wild-type mice (**Supplementary Fig. 3a**). No significant difference was observed in the morphine-induced analgesic effect in the TFR between the α3$^{-/-}$ mice and wild-type littermates (**Fig. 6e**). Moreover, there was no significant difference in the THC-induced analgesic effect in the TFR between the α2 GlyR subunit knockout mice (α2$^{-/-}$) and wild-type littermates (**Fig. 6f**). While CB1$^{-/-}$ mice showed no hypothermia after injection of the THC even at a high concentration (50 mg kg^{-1}), the THC-induced hypothermia did not significantly differ between the α3$^{-/-}$ and wild-type mice (**Supplementary Fig. 3c**). We next examined the effects of 5-desoxy-THC and di-desoxy-THC on body temperature and locomotor activity in C57BL/6J mice. Both 5-desoxy-THC and di-desoxy-THC when administrated alone did not significantly affect locomotor activity and body temperature of the mice (**Supplementary Fig. 3d,e**). Di-desoxy-THC at 20 mg kg^{-1} did not significantly alter THC (10 mg kg^{-1})-induced hypothermia and hypolocomotor activity in the mice (**Supplementary Fig. 3d,e**). However, both of these behavioral changes induced by THC were completely restored by administration of AM251 at 3 mg kg^{-1} respectively.

While the TFR represents a spinal reflex, the hot plate test is considered to involve supraspinal processing[20]. We next measured the analgesic effect of THC and 5-desoxy-THC in the hot plate test. Consistent with previous studies[2], THC increased response latency in the hot plate test (**Supplementary Fig. 4a**). THC-induced analgesia was prevented by administration of AM251 but not by strychnine and di-desoxy-THC (**Supplementary Fig. 4a**). In contrast to the observation in the TFR, 5-desoxy-THC was ineffective in producing an analgesic effect in the hot plate test in the wild-type, α3$^{-/-}$, CB1$^{-/-}$ and CB2$^{-/-}$ mice (**Supplementary Fig. 4b–d**). The extent of increase in response latency by THC did not significantly differ between the α3$^{-/-}$ mice and the wild-type littermates (**Supplementary Fig. 4b**). Consistent with a previous report[2], the THC-induced analgesic effect in the hot plate test was completely absent in the CB1$^{-/-}$ mice but not in the CB2$^{-/-}$ mice (**Supplementary Fig. 4c,d**).

Several recent studies have shown that HU 210 (**15**), a synthetic CB1-receptor full agonist structurally similar to THC (**Supplementary Fig. 5a**), can potentiate I_{Gly} in HEK 293 cells expressing recombinant GlyRs[11,12]. In view of this, we examined the analgesic effect of HU 210 in the TFR in CB$^{-/-}$ mice. Intraperitoneal administration of HU 210 20 min before the TFR produced analgesia in a dose-dependent manner from 3 mg kg^{-1} to 50 mg kg^{-1} in CB1$^{-/-}$ mice (**Supplementary Fig. 5b**). In these mice, the extent of HU 210–induced analgesia in the TFR was slightly less than that of THC. The magnitude of the analgesic effect induced by HU 210 (10 mg kg^{-1}, i.p.) reached its maximum 20–30 min after drug injection and substantially reduced 50 min after drug injection (**Supplementary Fig. 5c**). Di-desoxy-THC at 30 mg kg^{-1} significantly reduced the analgesic effect of HU 210 at 30 mg kg^{-1} in the TFR in CB$^{-/-}$ mice (**Supplementary Fig. 5d**). Strychnine at 0.2 mg kg^{-1}, subcutaneous (s.c.) completely abolished the HU 210–induced analgesic effect in the TFR. Consistent with a previous study[2], HU 210 did not cause hypothermia and analgesia in the hot plate test in CB$^{-/-}$ mice (**Supplementary Fig. 5e,f**).

DISCUSSION

We have identified a physical site critical for the THC-induced potentiating effect on I_{Gly} through functional mutagenesis of GlyRs. This conclusion is supported by the finding from NMR chemical shift measurements of the purified transmembrane domains of the α1 GlyR protein. THC is likely to interact with GlyRs through a hydrogen-bond interaction. This idea is consistent with previous studies of alcohol and anesthetic modulation of $GABA_A$ and glycine receptors. A cluster of polar amino acids in the TM2 and TM3 domains of these receptors have been found to play key roles in determining the receptor's sensitivity to various alcohols and anesthetics[21,22]. Alternately, the antagonism of di-desoxy-THC against a THC-induced potentiating effect suggests that there are hydrophobic residues in the vicinity of transmembrane domains of GlyR that also contribute to THC modulation of GlyRs. The antagonism of di-desoxy-THC appeared to be selective for the THC-induced but not propofol-induced potentiating effect on I_{Gly}. The simplest explanation is that a cavity exists among the transmembrane regions of GlyRs that may accommodate cannabinoids. There is a possibility that di-desoxy-THC may be a competitive inhibitor of the THC-induced effect if the concentrations of THC are high enough to overcome di-desoxy-THC. We had to set the cutoff concentration of both chemical compounds at 30 μM because of a solubility problem.

The results of the NMR chemical shift measurement favor a direct interaction between THC and residue Ser296 of GlyR-TM3. Chemical shift changes indicate changes in the electronic environment of the nuclei. The results from our titration experiments suggest that the environment near Ser296 is sensitively modulated by THC in a dose-dependent manner. Consistent with this, THC at low concentrations enhanced the function of the α1 and α3 GlyRs. Overall, these findings are not hard proof of a direct interaction but rather favor the simple explanation that a THC-GlyR interaction occurs in the vicinity of Ser296. THC is also likely to enhance GlyR channel

activity through an allosteric mechanism, given the observation that the S296A-S307A mutations of the α1 and α3 subunits altered the efficacy but not the apparent affinity (EC_{50}) of THC potentiation of I_{Gly}. The potency of a positive modulator may be more a function of ligand efficacy than affinity. This idea has been true with regard to many known allosteric modulators of GlyRs including alcohols and general anesthetics. It should be pointed out that several factors could prevent us from determining the precise EC_{50} values of THC potentiation in electrophysiological experiments. These factors include agonist concentrations, receptor desensitization, drug solubility, receptor density and posttranslational modulation of receptor protein. Among these factors, the problem with cannabinoid solubility indeed limited our ability to obtain precise assessment of the EC_{50} and E_{max} of THC concentration response curve in the mutant receptors.

On the basis of the data presented in this study, we propose that the THC-induced analgesia in the TFR is likely mediated via a mechanism dependent on the α3 GlyRs. In contrast, the analgesia of THC in the hot plate test is predominantly mediated by CB1 receptors, suggesting that the TFR and the hot plate effect are mediated through distinct mechanisms. A spinal component is proposed to critically contribute to the mechanism underlying THC-induced analgesia in the TFR in mice[2,23]. This correlates well with the observation that the α3 GlyRs are abundantly expressed in the dorsal horn of the spinal cord and is consistent with recent findings that spinal CB1 receptors may exert a pronociceptive action[6,7]. However, several previous studies reported that pretreatment with a selective CB1 receptor antagonist, SR141716A (**16**), inhibited THC-induced analgesic effect in the TFR in mice[5,24,25]. There are several factors that could account for the discrepancy between our study and previous studies. For instance, SR141716A at pharmacological doses greater than 3 mg kg^{-1} has been shown to produce direct effects on locomotor activity and body temperature[5,24], AM251 used in our study did not significantly alter either behavior. In addition, different strains of mice were used in our (C57BL/6J) and previous studies (ICR). Mice with different genetic backgrounds may differ in their response to the THC-induced analgesic effect as well as other cannabimimetic side effects such as hypolocomotion, hypothermia and psychosis. These behavior alterations can further complicate the assessment of the THC analgesia[26]. Another contributing factor is the setting of the test parameters in the TFR test, such as tail-flick latency of control group. Different tail-flick latencies (1 s versus 4 s) used across laboratories could, therefore, contribute to some conflicting observations of THC-induced analgesia in the TFR test in $CB1^{-/-}$ mice[2,27]. The α3 GlyRs are thought to be an essential target for chronic inflammatory pain induced by PGE_2 and other nonpainful stimuli[28,29]. It remains to be determined whether or not GlyRs could contribute to the therapeutic mechanisms of THC in the treatment of pathological pain. The role of the α1 GlyRs in cannabis-induced analgesia is unknown because we lack selective antagonists of GlyR subtypes and an ideal animal model[30].

Consistent with previous studies[10,11], detectable potentiation of I_{Gly} by THC was observed at low concentrations (30–300 nM) in cultured neurons and in HEK 293 cells expressing the α1 and α3 subunits. This concentration range is in line with human plasma concentrations (400–500 nM) of THC at 10 min after smoking two cigarettes[31]. The maximal magnitude of THC potentiation required continuous incubation of the drug for 3–5 min. A similar scenario has been described in cannabinoid modulation of 5-HT_3 and nicotinic acetylcholine (nACh) receptors, close members of GlyRs in a ligand-gated ion channel superfamily[32,33]. Because the E_{max} concentrations of THC potentiation were significantly increased, the EC_{50} values of THC potentiation of GlyRs were obtained in a lower micromolar range instead of the higher nanomolar range described previously[10,11]. One can argue about the clinical relevance of THC potentiation of I_{Gly}. It should be pointed out that the THC concentrations in brain and spinal tissues are found to be at least three–fourfold higher than plasma THC concentrations, according to a study in mice[25]. Moreover, the THC concentration is credible for the measurement of the cannabis-induced psychoactive effects but less important for the cannabis-induced analgesia. Among 480 components of cannabis sativa, 65 are structurally related compounds, namely phytocannabinoids. Many of these cannabinoids with weak or no psychoactivity have therapeutic potentials. For instance, cannabidiol (**17**), which is structurally similar to THC, has been used for the treatment of chronic pain in animals and human[9]. A recent study has shown that cannabidiol can enhance GlyR function in a manner similar to THC[34]. The concentrations of cannabidiol could be equal or close to the average concentrations of THC, which is estimated to be around 1–3% in overall cannabis preparations[31]. It is plausible to predict that the GlyRs could mediate some behavioral effects induced by other phytocannabinoids structurally similar to THC and cannabidiol. A previous observation that the analgesia of HU 210 in the TFR was absent in $CB1^{-/-}$ mice[2] is contradictory with our finding in this study. This discrepancy could be because different time points were used to measure the analgesic effect of HU 210 in the TFR after drug injection. We observed that the extents of THC- and HU 210–induced analgesia reached its maximum within 20 min after drug injection and declined significantly 50 min after drug injections. The time course of THC-induced analgesia is consistent with cannabinoid pharmacokinetics measured in mice and humans[25,31]. For instance, the peak concentration of THC occurred at 9 min in human plasma after smoking cannabis[31].

The widespread medical use of cannabis has been the topic of many debates in the last few decades, extending beyond the medical and scientific communities. This topic has been so controversial because the plant can produce effects beyond the therapeutic. It is important to identify distinct mechanisms that underlie the therapeutic effects induced by cannabis via non-CB1 pathways. The mechanism of THC-GlyR interaction revealed in this study not only enhances our understanding of the role of GlyRs in cannabis-induced analgesia but also promotes a new avenue for developing analgesic agents. For instance, 5-desoxy-THC appears to be one of the enticing candidates that produce an analgesic effect without causing a psychoactive effect. Except for antinociceptive action, cannabinoids and GlyRs play similar roles in the processes of neuromotor activity, seizure, anxiety, drugs of abuse and muscle relaxation[1,35]. The α1 and α3 GlyRs are abundantly expressed in many brain regions[13,36]. Our findings here also open up an opportunity to develop new genetically modified mice, which together with 5-desoxy-THC and di-desoxy-THC could be valuable for exploring the role of GlyRs in some of the nonpsychotropic cannabinoid-induced behaviors in future studies.

Collectively, these findings have revealed the molecular basis of THC potentiation of GlyRs and the role of GlyRs in some of cannabis-induced behaviors. The new mechanism underlying THC potentiation and certain types of cannabinoid-induced analgesia can potentially lead to a strategy for the development of a new class of analgesic agents.

METHODS

Animals. All behavioral experiments were conducted in male C57BL/6J mice unless otherwise indicated. The α3 $Glra^{+/-}$ mice were bred with each other to generate experimental animals: wild-type, α3 $Glra^{+/-}$ and α3 $Glra^{-/-}$ littermates. The $CB1^{-/-}$, $CB2^{-/-}$ and α2 $Glra^{-/-}$ mice were generated as previously described[2,37,38]. The homozygous mutants of the mice listed above were backcrossed into the C57BL/6J background for at least six generations and genotyped using primers given in the **Supplementary Methods**.

Cultured spinal neurons. PN0 rats were killed by cervical dislocation. The spinal cords were removed from three to five rats. Spinal neurons were plated at 300,000 cells per ml into 35-mm tissue culture dishes coated with poly-D-lysine (0.1 mg ml^{-1}). The neuronal feeding medium consisted of 90% minimal essential medium, 10% (v/v) heat-inactivated FBS and a mixture of nutrient supplements (Invitrogen).

HEK 293 cell transfection and recording. HEK 293 cells were cultured as described previously[39]. The plasmid cDNAs of the wild-type and mutant GlyR subunits were transfected using the SuperFect Transfection Kit (Qiagen). The currents were recorded 1–2 days after transfection. HEK 293 cells but not neurons were lifted and continuously recorded as described previously[33].

Immunoblot of membrane surface proteins. Immunoblot of the surface and total α1 GlyR proteins expressed in HEK 293 cells were conducted following a procedure described previously[33]. A polyclonal antibody (1:200) directed to the extracellular N-terminal domain of the GlyR (Sigma, catalog number G0666) was used to detect the α1 GlyR proteins. Blots were developed using Supersignal West Pico Chemiluminescent Substrate or SuperSignal West Dura Extended Duration Substrate (Pierce). A Kodak DC290 camera was used to capture field images. Protein bands were analyzed using ImageJ software (http://rsb.info.nih.gov/ij/).

Molecular modeling. Human α1 GlyR is homology modeled with SWISS-MODEL[40], using 3EHZ PDB structure chain A as a template[41]. The N-terminal extracellular domain (1–214) was removed. The 69-residue peptide of the intracellular loop connecting the TM3 and TM4 domains was replaced by a 7-residue linker, REFGGGG. Five α1 GlyR chains were superimposed on the five chains in 3EHZ to create a pentamer conformation and then energy minimized for 10,000 steps.

NMR spectroscopy. The full-length transmembrane domains of the α1 GlyR for NMR binding studies were prepared using the established method as detailed previously[42–44] and outlined in the **Supplementary Methods**. Rosetta(DE3) pLysS competent *E. coli* cells (Novagen) were used to express the protein in the M9 medium for uniform ^{15}N-labeling or ^{15}N, ^{13}C–double labeling. Protein samples were prepared in two concentrations, 250 μM and 450 μM, in LPPG micelles with a 10-mM sodium phosphate buffer (pH 5.8). Three titration experiments, with low and high ligand-to-protein ratios for THC effects and ethanol effects, were performed. The experiments with high ligand-to-protein ratio were performed after the GlyR-TM sample was titrated with 0.2% ethanol except for the first point. All titrations were prepared from a stock solution of 32 mM THC in ethanol. The highest THC concentration titrated was 96 μM. The chemical shift changes reported here are weighted averages calculated using the equation $\Delta\delta = \sqrt{(\Delta H)^2 + (\frac{\Delta N}{5})^2}$, where ΔH and ΔN are the Ser296 amide proton and amide nitrogen chemical shift changes, respectively, after titrations of THC.

Site-directed mutagenesis. Point mutations of the human α1 GlyR, rat α2 and α3 GlyR subunits were introduced using a QuikChange Site-Directed Mutagenesis Kit (Stratagene). The authenticity of the DNA sequence through the mutation sites was confirmed by double-stranded DNA sequencing using a Cequation (8000) Genetic Analysis System (Beckman Coulter, Inc).

[^{3}H]-CP55940 binding of CB1 and CB2 receptors. Mouse brain tissues (CB1) and Rosetta(DE3) pLysS competent *E. coli* cells (Novagen) transfected with human CB2 receptor cDNA were collected and homogenized using Brickman polytron homogenizer at 500 r.p.m. for 30 s in ice cold 50 mM Tris-HCl, EDTA 1 mM, $MgCl_2$ 3 mM, pH 7.4. The homogenate was centrifuged at 48,000*g* for 20 min at 4 °C. The membrane pellet was suspended and incubated with various concentrations of [^{3}H]-CP55940 (PerkinElmer) in PBS containing 0.2% (w/v) BSA at 30 °C for 60 min. Nonspecific binding was determined in the presence of 1 μM of CP55940. Bound and free [^{3}H]-CP55940 was separated by rapid vacuum filtration in a Brandell harvester through GF/B filters. The filters were washed four times with 4 ml cold PBS containing 0.1% (w/v) BSA. The filters were punched into scintillation vials containing 5 ml liquid scintillation cocktail. The samples were counted in a scintillation counter at 50% efficiency. Assays were performed in triplicate, and each experiment was repeated at least three times.

[^{35}S]-GTP-γs binding. The membrane proteins of the mouse brains were prepared following the protocol described above. The membrane pellet was suspended in [^{35}S]-GTP-γs binding reaction buffer, which contains 50 mM Tris-HCl, 0.2 mM EGTA, 9 mM $MgCl_2$, 150 mM NaCl, 50 μM GDP and 1.4 mg ml^{-1} BSA. The membranes were incubated with 0.5 nM [^{35}S]-GTP-γs for 2 h at 30 °C. The filters were washed twice with 4 ml cold 10 mM Tri-HCl. Nonspecific binding was determined by 40 μM of GTP-γs. Bound and free [^{35}S]-GTP-γs was separated by rapid vacuum filtration in a Brandell harvester through GF/B filters.

Tail-flick reflex test. Mice responded to a focused heat stimulus by flicking or moving their tail from the path of the stimulus, thereby exposing a photocell located in the tail-flick analgesia meter (Ugo Basile Tail-flick Unit 7360) immediately below the tail. The reaction time was automatically recorded. Prior to dosing, the nociceptive threshold was measured three times, and the mean of the reaction times was used as baseline latency for each mouse. The cut-off time of 16 s was used to prevent tissue damage.

Drugs. The details of the drugs used in this study are given in the **Supplementary Methods**.

Received 3 August 2010; accepted 16 February 2011; published online 3 April 2011

References

1. Pacher, P., Batkai, S. & Kunos, G. The endocannabinoid system as an emerging target of pharmacotherapy. *Pharmacol. Rev.* **58**, 389–462 (2006).
2. Zimmer, A., Zimmer, A.M., Hohmann, A.G., Herkenham, M. & Bonner, T.I. Increased mortality, hypoactivity, and hypoalgesia in cannabinoid CB1 receptor knockout mice. *Proc. Natl. Acad. Sci. USA* **96**, 5780–5785 (1999).
3. Oz, M. Receptor-independent actions of cannabinoids on cell membranes: focus on endocannabinoids. *Pharmacol. Ther.* **111**, 114–144 (2006).
4. Zhang, L. & Xiong, W. Modulation of the Cys-loop ligand-gated ion channels by fatty acid and cannabinoids. *Vitam. Horm.* **81**, 315–335 (2009).
5. Welch, S.P., Huffman, J.W. & Lowe, J. Differential blockade of the antinociceptive effects of centrally administered cannabinoids by SR141716A. *J. Pharmacol. Exp. Ther.* **286**, 1301–1308 (1998).
6. Pernía-Andrade, A.J. *et al.* Spinal endocannabinoids and CB1 receptors mediate C-fiber-induced heterosynaptic pain sensitization. *Science* **325**, 760–764 (2009).
7. Zhang, G., Chen, W., Lao, L. & Marvizon, J.C. Cannabinoid CB1 receptor facilitation of substance P release in the rat spinal cord, measured as neurokinin 1 receptor internalization. *Eur. J. Neurosci.* **31**, 225–237 (2010).
8. Klein, T.W. & Newton, C.A. Therapeutic potential of cannabinoid-based drugs. *Adv. Exp. Med. Biol.* **601**, 395–413 (2007).
9. Izzo, A.A., Borrelli, F., Capasso, R., Di Marzo, V. & Mechoulam, R. Non-psychotropic plant cannabinoids: new therapeutic opportunities from an ancient herb. *Trends Pharmacol. Sci.* **30**, 515–527 (2009).
10. Hejazi, N. *et al.* Delta9-tetrahydrocannabinol and endogenous cannabinoid anandamide directly potentiate the function of glycine receptors. *Mol. Pharmacol.* **69**, 991–997 (2006).
11. Yang, Z. *et al.* Subunit-specific modulation of glycine receptors by cannabinoids and N-arachidonyl-glycine. *Biochem. Pharmacol.* **76**, 1014–1023 (2008).
12. Demir, R. *et al.* Modulation of glycine receptor function by the synthetic cannabinoid HU210. *Pharmacology* **83**, 270–274 (2009).
13. Lynch, J.W. Native glycine receptor subtypes and their physiological roles. *Neuropharmacology* **56**, 303–309 (2009).
14. Shiang, R. *et al.* Mutational analysis of familial and sporadic hyperekplexia. *Ann. Neurol.* **38**, 85–91 (1995).
15. Shiang, R. *et al.* Mutations in the alpha 1 subunit of the inhibitory glycine receptor cause the dominant neurologic disorder, hyperekplexia. *Nat. Genet.* **5**, 351–358 (1993).
16. Harvey, R.J. *et al.* GlyR alpha3: an essential target for spinal PGE2-mediated inflammatory pain sensitization. *Science* **304**, 884–887 (2004).
17. Griffon, N. *et al.* Molecular determinants of glycine receptor subunit assembly. *EMBO J.* **18**, 4711–4721 (1999).
18. Jordt, S.E. *et al.* Mustard oils and cannabinoids excite sensory nerve fibres through the TRP channel ANKTM1. *Nature* **427**, 260–265 (2004).
19. Kimura, T., Cheng, K., Rice, K.C. & Gawrisch, K. Location, structure, and dynamics of the synthetic cannabinoid ligand CP-55,940 in lipid bilayers. *Biophys. J.* **96**, 4916–4924 (2009).
20. Grossman, M.L., Basbaum, A.I. & Fields, H.L. Afferent and efferent connections of the rat tail flick reflex (a model used to analyze pain control mechanisms). *J. Comp. Neurol.* **206**, 9–16 (1982).
21. Lobo, I.A. & Harris, R.A. Sites of alcohol and volatile anesthetic action on glycine receptors. *Int. Rev. Neurobiol.* **65**, 53–87 (2005).
22. Harris, R.A., Trudell, J.R. & Mihic, S.J. Ethanol's molecular targets. *Sci. Signal.* **1**, re7 (2008).
23. Smith, P.B. & Martin, B.R. Spinal mechanisms of delta 9-tetrahydrocannabinol-induced analgesia. *Brain Res.* **578**, 8–12 (1992).
24. Compton, D.R., Aceto, M.D., Lowe, J. & Martin, B.R. In vivo characterization of a specific cannabinoid receptor antagonist (SR141716A): inhibition of delta 9-tetrahydrocannabinol-induced responses and apparent agonist activity. *J. Pharmacol. Exp. Ther.* **277**, 586–594 (1996).
25. Varvel, S.A. *et al.* Delta9-tetrahydrocannbinol accounts for the antinociceptive, hypothermic, and cataleptic effects of marijuana in mice. *J. Pharmacol. Exp. Ther.* **314**, 329–337 (2005).
26. Marris, E. More pain studies needed. *Nature* **458**, 394–395 (2009).
27. Ledent, C. *et al.* Unresponsiveness to cannabinoids and reduced addictive effects of opiates in CB1 receptor knockout mice. *Science* **283**, 401–404 (1999).
28. Zeilhofer, H.U. The glycinergic control of spinal pain processing. *Cell. Mol. Life Sci.* **62**, 2027–2035 (2005).
29. Zeilhofer, H.U. Prostanoids in nociception and pain. *Biochem. Pharmacol.* **73**, 165–174 (2007).
30. Findlay, G.S. *et al.* Glycine receptor knock-in mice and hyperekplexia-like phenotypes: comparisons with the null mutant. *J. Neurosci.* **23**, 8051–8059 (2003).
31. Huestis, M.A. Human cannabinoid pharmacokinetics. *Chem. Biodivers.* **4**, 1770–1804 (2007).

32. Spivak, C.E., Lupica, C.R. & Oz, M. The endocannabinoid anandamide inhibits the function of alpha4beta2 nicotinic acetylcholine receptors. *Mol. Pharmacol.* **72**, 1024–1032 (2007).
33. Xiong, W., Hosoi, M., Koo, B.N. & Zhang, L. Anandamide inhibition of 5–HT3A receptors varies with receptor density and desensitization. *Mol. Pharmacol.* **73**, 314–322 (2008).
34. Ahrens, J. *et al.* The nonpsychotropic cannabinoid cannabidiol modulates and directly activates alpha-1 and alpha-1-Beta glycine receptor function. *Pharmacology* **83**, 217–222 (2009).
35. Laube, B., Maksay, G., Schemm, R. & Betz, H. Modulation of glycine receptor function: a novel approach for therapeutic intervention at inhibitory synapses? *Trends Pharmacol. Sci.* **23**, 519–527 (2002).
36. Delaney, A.J., Esmaeili, A., Sedlak, P.L., Lynch, J.W. & Sah, P. Differential expression of glycine receptor subunits in the rat basolateral and central amygdala. *Neurosci. Lett.* **469**, 237–242 (2010).
37. Buckley, N.E. *et al.* Immunomodulation by cannabinoids is absent in mice deficient for the cannabinoid CB(2) receptor. *Eur. J. Pharmacol.* **396**, 141–149 (2000).
38. Young-Pearse, T.L., Ivic, L., Kriegstein, A.R. & Cepko, C.L. Characterization of mice with targeted deletion of glycine receptor alpha 2. *Mol. Cell. Biol.* **26**, 5728–5734 (2006).
39. Hu, X.Q., Zhang, L., Stewart, R.R. & Weight, F.F. Arginine 222 in the pre-transmembrane domain 1 of 5–HT3A receptors links agonist binding to channel gating. *J. Biol. Chem.* **278**, 46583–46589 (2003).
40. Arnold, K., Bordoli, L., Kopp, J. & Schwede, T. The SWISS-MODEL workspace: a web-based environment for protein structure homology modelling. *Bioinformatics* **22**, 195–201 (2006).
41. Hilf, R.J. & Dutzler, R. Structure of a potentially open state of a proton-activated pentameric ligand-gated ion channel. *Nature* **457**, 115–118 (2009).
42. Canlas, C.G., Cui, T., Li, L., Xu, Y. & Tang, P. Anesthetic modulation of protein dynamics: insight from an NMR study. *J. Phys. Chem. B* **112**, 14312–14318 (2008).
43. Ma, D., Liu, Z., Li, L., Tang, P. & Xu, Y. Structure and dynamics of the second and third transmembrane domains of human glycine receptor. *Biochemistry* **44**, 8790–8800 (2005).
44. Tang, P., Mandal, P.K. & Xu, Y. NMR structures of the second transmembrane domain of the human glycine receptor alpha(1) subunit: model of pore architecture and channel gating. *Biophys. J.* **83**, 252–262 (2002).

Acknowledgments

We thank C.L. Cepko for providing $\alpha 2^{-/-}$ Glra mice. We especially thank D.M. Lovinger for critical comments on the manuscript. This work was supported by funds from the intramural program of the US National Institute on Alcohol Abuse and Alcoholism. We acknowledge the grant support (R37GM049202 to Y.X.) from the US National Institute of General Medical Sciences of the US National Institutes of Health.

Author contributions

W.X. and L.Z. designed and conducted electrophysiology, biochemical and biophysical experiments and animal behavioral tests. K.-J.C. and K.C.R. synthesized cannabinoid chemicals. T-X.C. and Y.X. conducted protein expression, purification and NMR experiments of the full-length transmembrane domains of the α1 GlyR and carried out NMR analysis. G.G. conducted animal behavioral tests. L.Z. supervised the project and wrote the manuscript. Y.X. critically revised the manuscript.

Competing financial interests

The authors declare no competing financial interests.

Additional information

Supplementary information and chemical compound information is available online at http://www.nature.com/naturechemicalbiology/. Reprints and permissions information is available online at http://npg.nature.com/reprintsandpermissions/. Correspondence and requests for materials should be addressed to L.Z.